Protist, Vol. 167, 279–301, June 2016
http://www.elsevier.de/protis
Published online date 17 May 2016

Protist

ORIGINAL PAPER

Morphology and Molecular Phylogeny of Coelomic Gregarines (Apicomplexa) with Different Types of Motility: *Urospora ovalis* and *U. travisiae* from the Polychaete *Travisia forbesii*

Andrei Diakin[a,1], Gita G. Paskerova[b,1], Timur G. Simdyanov[c], Vladimir V. Aleoshin[d], and Andrea Valigurová[a]

[a]Department of Botany and Zoology, Faculty of Science, Masaryk University, Kotlářská 2, 611 37, Brno, Czech Republic
[b]Department of Invertebrate Zoology, Faculty of Biology, St. Petersburg State University, Universitetskaya emb. 7/9, Saint-Petersburg, 199 034, Russian Federation
[c]Department of Invertebrate Zoology, Faculty of Biology, Lomonosov Moscow State University, Leninskie Gory, Moscow 119 234, Russian Federation
[d]Belozersky Institute for Physico-Chemical Biology, Lomonosov Moscow State University, Leninskie Gory, Moscow 119 234, Russian Federation

Submitted November 18, 2015; Accepted May 5, 2016
Monitoring Editor: C. Graham Clark

Urosporids (Apicomplexa: Urosporidae) are eugregarines that parasitise marine invertebrates, such as annelids, molluscs, nemerteans and echinoderms, inhabiting their coelom and intestine. Urosporids exhibit considerable morphological plasticity, which correlates with their different modes of motility and variations in structure of their cortical zone, according to the localisation within the host. The gregarines *Urospora ovalis* and *U. travisiae* from the marine polychaete *Travisia forbesii* were investigated with an emphasis on their general morphology and phylogenetic position. Solitary ovoid trophozoites and syzygies of *U. ovalis* were located free in the host coelom and showed metabolic activity, a non-progressive movement with periodic changes of the cell shape. Solitary trophozoites of *U. travisiae*, attached to the host tissue or free floating in the coelom, were V-shaped. Detached trophozoites demonstrated gliding motility, a progressive movement without observable cell body changes. In both gregarines, the cortex formed numerous epicytic folds, but superfolds appeared exclusively on

[1]Corresponding authors;
e-mail diakin@sci.muni.cz (A. Diakin), gitapasker@yahoo.com (G.G. Paskerova).

http://dx.doi.org/10.1016/j.protis.2016.05.001
1434-4610/© 2016 Elsevier GmbH. All rights reserved.

the surface of *U. ovalis* during metabolic activity. SSU rDNA sequences obtained from *U. ovalis* and *U. travisiae* revealed that they belong to the Lecudinoidea clade; however, they are not affiliated with other coelomic urosporids (*Pterospora* spp. and *Lithocystis* spp.), but surprisingly with intestinal lecudinids (*Difficilina* spp.) parasitising nemerteans.
© 2016 Elsevier GmbH. All rights reserved.

Key words: Urosporidae; marine eugregarines; ultrastructure; gliding and metaboly; superfolds; 18S rDNA phylogeny.

Introduction

Apicomplexa Levine 1980, emend. Adl et al. 2012 (Adl et al. 2012) consist entirely of unicellular organisms parasitising various animals. Some of them cause important human and domestic animal diseases (e.g. malaria, toxoplasmosis, and cryptosporidiosis); therefore, these species have been intensively studied in different aspects of biology, medicine and phylogeny. However, basal apicomplexans (e.g. gregarines, agamococcidia, blastogregarines, and protococcidia), inhabiting exclusively invertebrate hosts, are crucial for our understanding of the evolutionary pathways of Apicomplexa, yet they still remain poorly investigated. Gregarines parasitise a broad range of terrestrial and aquatic invertebrates (annelids, turbellarians, arthropods, echinoderms, and urochordates), and inhabit different sites within the host organism, e.g. the gut and its derivatives (the Malpighian tubules, respiratory trees), the body cavity, and the reproductive system.

According to their morphological features, life cycles, and host range, gregarines are usually subdivided into three groups: Archigregarinorida Grassé, 1953, Eugregarinorida Léger 1900, and Neogregarinorida Grassé, 1953 (Adl et al. 2012; Desportes and Schrével 2013; Grassé 1953; Perkins et al. 2000). In contrast to coccidia, developmental stages of gregarines are predominantly extracellular and of large dimensions. The feeding stages (trophozoites) of gregarines are usually motile and heteropolar, with opposite ends differing in their structure and function. Usually gregarines undergo their vegetative phase of development when attached to the host tissue; the majority of them lack the form of asexual reproduction called merogony (=schizogony). Another important characteristic of the gregarine life cycle is the presence of a pre-sexual association, the so-called syzygy, usually consisting of two partners. There are several types of syzygies: caudo-frontal (head-to-tail), frontal (head-to-head), caudal (tail-to-tail), and lateral (partners are in contact at their lateral surfaces). In the majority of eugregarines and archigregarines, the partners in the syzygies retain the motility characteristic of solitary trophozoites. In the course of time, the partners become hemispherical in shape, form a common envelope (a gametocyst wall), and undergo gametogenesis, followed by sporogenesis (Desportes and Schrével 2013; Grassé 1953; Perkins et al. 2000).

Gregarines show a great variety of cell shapes and different modes of motility that seem to correlate with trophozoite localisation within the host. Gregarines from the intestine are generally vermiform (archigregarines) and demonstrate pendular (rolling) motility, or elongated (most eugregarines) and show gliding motility. Parasites from the body cavity, tissues, or the reproductive system are usually oval or roundish (some of the urosporids and monocystids), or dendritic (*Pterospora* spp.). As a rule, such gregarines possess metabolic or peristaltic motility (*Nematopsis magna*, *Lithocystis schneideri, Urospora neapolitana*); some of them are non-motile (*Gonospora varia*, *Lythocystis foliaceae*, *Urospora chiridotae*) (Coulon and Jangoux 1987; Desportes and Schrével 2013; Dyakin and Paskerova 2004; Dyakin and Simdyanov 2005; Frolov 1991; Landers and Gunderson 1986; Levine 1977; MacMillan 1973; Miles 1968; Perkins et al. 2000; Schrével 1964, 1971a, b, and others). While gliding is a progressive movement, both pendular (rolling) and metaboly are non-progressive. In addition, metaboly is accompanied with periodic changes of the cell body shape.

The exact mechanism of gregarine motility remains unknown. Gliding motility seems to be facilitated by the complex organisation of the parasite's cortical zone. The pellicle forms longitudinal epicytic folds with special sets of filamentous structures in their apex (the so-called rippled dense structures [RDS and 12-nm apical filaments) and an internal lamina, which underlays the inner membrane complex (IMC) (Schrével et al. 1983; Vivier 1968). The polymerised form of actin and cytoplasmic mucus, excreted outside the cell, both actively participate in gregarine gliding (Valigurová et al.

2013). Peristaltic or metabolic motility is accompanied by the forming of one or several contracted regions running from one end to the other along the longitudinal axis of the cell. It was assumed that this type of motility can be facilitated by the presence of a subpellicular cytoskeletal network; however, its nature, whether it is composed of fibrils or microtubules, remains unknown (MacMillan 1973; Warner 1968).

The family Urosporidae, established by L. Léger (Léger 1892), combining the monocystid gregarines with heteropolar oocysts, nowadays comprises several genera of parasites inhabiting various marine and freshwater invertebrates (mainly echinoderms and polychaetes, as well as oligochaetes, sipunculids, molluscs, nemerteans) (Desportes and Schrével 2013; Dogiel 1906, 1909, 1910; Grassé 1953, Levine 1977; Perkins et al. 2000; Pixell-Goodrich 1915, 1950). To date, most investigations concerning urosporids are either faunistic studies or morphological descriptions of various developmental stages (mostly trophozoites and oocysts), performed at light microscopic level. Only a few members have been studied from an ultrastructural viewpoint (Corbel et al. 1979; Dyakin and Simdyanov 2005; Landers and Leander 2005; Pomory and Lares 1998), and even fewer have been investigated at the molecular biological level (Leander et al. 2006).

The type genus *Urospora* Schneider, 1895 unites monocystid gregarines from the body cavity or tissues of hosts, with lateral or frontal syzygies, and with heteropolar oocysts possessing a thin appendage at one end and a conical transparent funnel at the other (Desportes and Schrével 2013; Grassé 1953; Levine 1977). In the present study, we investigated the morphology and molecular phylogeny of gregarines of two closely related urosporid species *Urospora ovalis* Dogiel, 1910 and *U. travisiae* Dogiel, 1910, parasites of the body cavity of the marine polychaete *Travisia forbesii* Johnston, 1840, noting, in addition, the biodiversity and adaptations of gregarines from coelomic habitats.

Results

All dissected hosts (approx. 400 individuals) were infected with *Urospora ovalis* and *Urospora travisiae* (Fig. 1A). The parasites inhabited the host body cavity. In addition, spherical gametocysts with typical urosporid oocysts were found. The oval-shaped oocysts were heteropolar, with a funnel and a tail at opposite ends, and about 20 μm (n = 40) in length, 7 μm (n = 40) in width (Fig. 1A, inset).

The intensity of parasitisation by both gregarine species varied during the summer season. In the case of *U. ovalis*, it reached up to 50 parasites per host in June/July, while no more than 5 in August/early September. In the case of *U. travisiae*, it also reached up to 50 parasites per host (in rare cases, no more than 5) during the entire summer season. For *U. ovalis*, both solitary trophozoites (June/August) and syzygies (August/early September) were found, while for *U. travisiae*, mostly solitary trophozoites were observed, and syzygies were found in a few cases only.

The main species characteristics of *U. ovalis* and *U. travisiae* are summarised in Table 1.

General Morphology and Ultrastructure of *Urospora ovalis*

The solitary trophozoites of *U. ovalis*, occurring freely in the host body cavity, were ovoid with rounded ends and showed no signs of heteropolarity under the light microscope (LM) (Fig. 1A-D). The cell size varied widely: 19.6 - 294.0 μm (av. 179 μm, mode 252 μm, n = 36) in length and 12.6 - 187.6 μm (av. 114 μm, mode 134 μm, n = 36) in width. We did not observe any young stages of *U. ovalis*.

Some parasites were glued to the host peritoneal epithelium by means of a mucous substance surrounding them. (Fig. 1B-C). Living parasites which had fallen out of the host during dissection showed characteristic metabolic (peristaltic) activity, during which cells alternately contracted at their ends causing the migration of the cytoplasm from one end to the other (Fig. 1D, Supplementary Material Video 1). Several superficial, longitudinal ridges formed in the contracted regions during gregarine movement. These ridges were visible even in histological sections (Fig. 1B-C).

Under SEM, these ridges corresponded to the so-called superfolds that run along the surface of the contracted region (Fig. 2A, C). However, during processing for electron microscopy (EM), solitary motile cells of *U. ovalis* completely contracted in most cases, and superfolds identical to those observed in contracted regions appeared on the entire gregarine surface (Fig. 2B, E). In transversal sections, both narrow (0.4-0.5 μm wide at the base) and wide (2.5-3.5 μm wide at the base) superfolds of uniform height (1 μm on average) were present at the surface of contracted cells (Fig. 3A-C).

The cells of *U. ovalis* were covered with a typical three-layered pellicle consisting of the plasma

Figure 1. Localisation of *Urospora ovalis* and *U. travisiae* in the polychaete *Travisia forbesii* and light microscopic observations of *U. ovalis* **A**. Sagittal section of the host infected with *U. ovalis* and *U. travisiae* (white arrowheads) located in the body cavity (bc). The black rectangles mark the parasites presented in Figure 1B (*U. ovalis*) and Figure 5A (*U. travisiae*) at high magnification. Ant – anterior end of the host, D – dorsal side of the host; il – intestinal lumen of the host, ph – pharynx; oo – oocytes of the host, Post – posterior end of the host, V – ventral side of the host. LM, H&E. The inset shows an oocyst with a funnel (f) and a tail (t) at opposite ends. LM. **B** – **C**. Histological sections of trophozoites of *U. ovalis* located in the host body cavity (bc), in different planes. Note mucous substance (ms) surrounded parasites and ridges (black arrows) at the parasite surface. oo – oocytes of the host. LM, H&E. **D**. Micrograph of the solitary *U. ovalis* trophozoite during cell metaboly. Note contracted region (black arrowheads) of the cell with ridges at the surface (black arrows). n – nucleus. PC. **E**. Syzygy of *U. ovalis.* Note ridges (black arrows) at free ends of gamonts. vac – vacuoles. BF.

membrane and the inner membrane complex (IMC). The pellicle formed numerous thin and waved epicytic folds (Fig. 2D). Their width was usually about 90 nm, while their height cyclically varied within the range from 0.5 to 1.4 μm. (Fig. 3B-C, E). The number of epicytic folds in 1 μm of the surface varied from 3 to 7, in dependence of the degree of cell contraction. The rippled dense structures and 12-nm apical filaments were not distinguishable; however, there was a single electron-dense rod located just beneath the IMC in the apical part of each epicytic fold (Fig. 3D-E). The 19-24 nm thick internal lamina underlay the IMC and formed curved bridges in the basal part of each fold, thereby separating the cytoplasm of folds from the rest of the gregarine cytoplasm (Fig. 3D-E). Under SEM the folds in non-contracted, as well as contracted regions were undulating or waving (Fig. 2D-E). Each superfold bore 10-20 epicytic folds (Fig. 3B-C).

Numerous cortical microtubules were arranged in transversal bundles located just beneath the pellicle. They did not form a continuous ring in the cell periphery, and some of the microtubules extended into the superfolds (Fig. 3B-D).

Typical apicomplexan micropores, appearing as short cylindrical invaginations of the plasma membrane terminated by a vesicle (about 55 nm in diameter), could occasionally be observed (Fig. 3F). The cylindrical part was enforced by an electron-dense collar (ca. 130 nm in diameter), formed by the IMC and the internal lamina. In addition, numerous structures resembling micropores (micropore-like structures) were located in the gregarine cortex between the epicytic folds (Fig. 3E, G-H). In these structures, the IMC and internal lamina formed an electron-dense cone-shaped collar situated beneath the intact plasma membrane (Fig. 3E, G). Numerous cytoplasmic vesicles (about 0.2 μm in diameter) filled with an electron-dense,

Table 1. Main species characters of *Urospora ovalis* and *U. travisiae*.

	Urospora ovalis	*Urospora travisiae*
Host	*Travisia forbesii*	
Localisation in the host	coelom	
Attachment to the host tissues	non-attached	attached
Cell shape	ovoid	V-like
Number of cell axis	1	2
Cell dimension (average, μm) of mature trophozoites	179 × 114	395 × 380 per branch
Cell motility	metaboly or peristalsis (non-progressive movement)	gliding (progressive movement)
Cell polarity	-	+
Attachment site	-	+
Cortex		
Epicytic folds	typical for gliding eugregarines	
Superfolds	+	-
Cytoplasm differentiation into ectoplasm and endoplasm	-	+
Oocysts	spindle-shaped, heteropolar, with a funnel and the hairy-tail at opposite ends	
Distribution	Barents Sea (Murmansk coast), White Sea (Karelian coast)	
References	Dogiel 1910; present study	

homogeneous material were usually situated in the vicinity of micropore-like structures as well as deeper within the parasite cytoplasm (Fig. 3B). Some of them were in contact with the collar. Except for a few cases, there was no fusion between these vesicles and the plasma membrane (Fig. 3G-H). The electron-dense droplets occasionally observed between the epicytic folds could be secreted by these vesicles (Fig. 3E).

There was no obvious division of cell cytoplasm into two zones, ectoplasm and endoplasm, as is typical for eugregarines. Many amylopectin granules were irregularly distributed in the cytoplasm, and several mitochondria could be observed at the cell periphery (Fig. 3A-C). The dictyosomes of Golgi apparatus, surrounded by numerous small and round vesicles, were mainly localised in the central zone of the cell (Fig. 3A).

The cytoplasm was packed with numerous and different structures, exhibiting a lower quantity at the cell periphery in comparison to the central cell region (Fig. 3A). Electron-dense, homogeneous inclusions of uncertain shape (di) accumulated predominantly around the nucleus. Some of them were in group of 2-3 and were usually accompanied by small transparent vesicles (Fig. 3A, I). Another type of inclusions was represented by large and round electron-transparent vacuoles (ov) with a loose filamentous content (Fig. 3A, J). In addition, electron-dense, roundish vacuoles (dv) with a heterogeneous granular content were found in the cytoplasm (Fig. 3A, K).

The eccentrically located nucleus possessed one large and several small nucleoli. The large nucleolus lay close to the nuclear envelope; the rest of the nucleoplasm was homogenous with a fine-grained content (Fig. 3A). This nucleolus consisted of two parts: the larger one was dense, homogeneous and directed towards the centre of the nucleus, while the smaller one was heterogeneous and faced the rough and two-layered nuclear envelope. There were several inclusions of nucleoplasm in both parts of the nucleolus (Fig. 3A).

Mature trophozoites (gamonts) in syzygies were connected to each other by their ends. The free ends of partners in syzygies were rounded (in rare cases) or bulb-shaped (in most cases). In the first case, syzygies showed active metabolic motility comparable with that of solitary parasites. In the second case, they moved much more slowly. In all cases, both partners demonstrated ridges on their surface in contracted regions (Fig. 1E), similar to those observed in moving solitary trophozoites (Fig. 1D). The gamonts in all of the observed

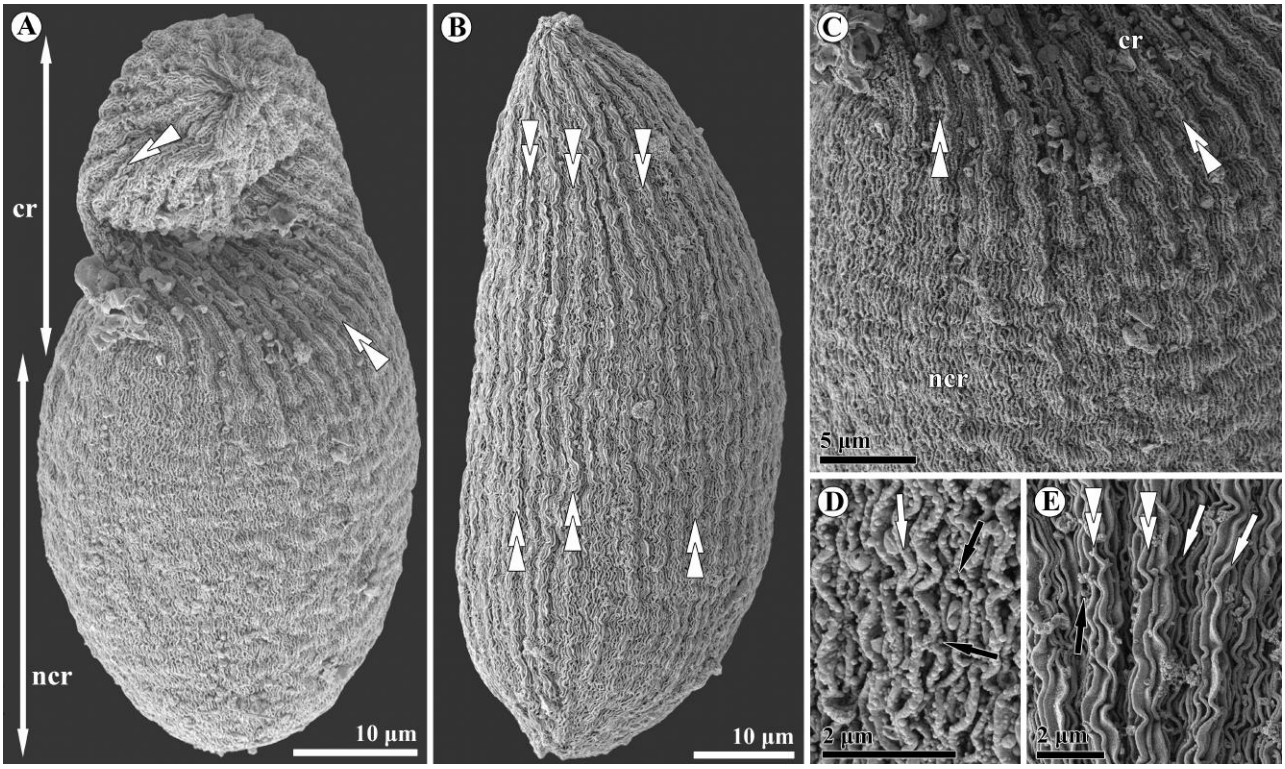

Figure 2. General morphology and surface ultrastructure of solitary *Urospora ovalis* trophozoites. **A**. General view of a trophozoite fixed during its movement. Contracted (cr) and non-contracted (ncr) regions are visible in the cell. White double arrowheads indicate superfolds. SEM. **B**. General view of a completely contracted trophozoite with superfolds (white double arrowheads) that ran over the entire cell surface. SEM. **C.** Detailed view of Figure 2A showing a transition between the contracted (cr) and non-contracted (ncr) regions of the cell. White double arrowheads mark superfolds in the contracted region. SEM. **D.** Details of epicytic folds (white arrow) covering the non-contracted region. Note electron-dense droplets (black arrow) located between the epicytic folds. SEM. **E.** Details of superfolds (white double arrowheads) and epicytic folds (white arrow) of a contracted cell. Black arrow points to an electron-dense droplet between epicytic folds. SEM.

syzygies were larger than solitary trophozoites, and their cytoplasm was completely filled with large transparent vacuoles (Fig. 1E).

During processing for EM, gamonts in syzygies changed their shape by rounding their free ends (Figs 1E vs. 4A). In contrast to solitary trophozoites, fixed gamonts had no superfolds on their surface (Figs 2A-C vs. 4A-C, Figs 3A-C vs. 4E). The height of epicytic folds in syzygies cyclically varied within the range from 0.7 to 2 μm, so that longitudinal sets of high epicytic folds alternating with lower ones were good visible on the syzygies surfaces (Fig. 4A-E). The number of epicytic folds in 1 μm of the surface varied from 3 to 5. There were droplets of mucus between these folds (Fig. 4C). Neither micropores, nor similar structures interrupting the cortex were found in all examined ultrathin sections (Fig. 4E).

The contact zone between two syzygy partners appeared simple, lacking an additional collar or other pellicle modifications (Fig. 4D). Usually, the sets of high epicytic folds of both partners coincided with each other (Fig. 4A, D). The free ends of gamonts in syzygy exhibited almost identical superficial morphology: they were slightly bulged-in (Fig. 4F-G).

The cytoplasm of syzygy partners was filled with a huge amount of electron- transparent vacuoles with loose filamentous content (Fig. 4E), similar to those found in solitary trophozoites (Fig. 3J, ov), but extremely enlarged in volume. Among them, there were many other inclusions such as lipid droplets and amylopectin granules. Electron-dense vacuoles and inclusions resembling the “di” and “dv” found in solitary trophozoites (Fig. 3I, K) were also observed (Fig. 4E).

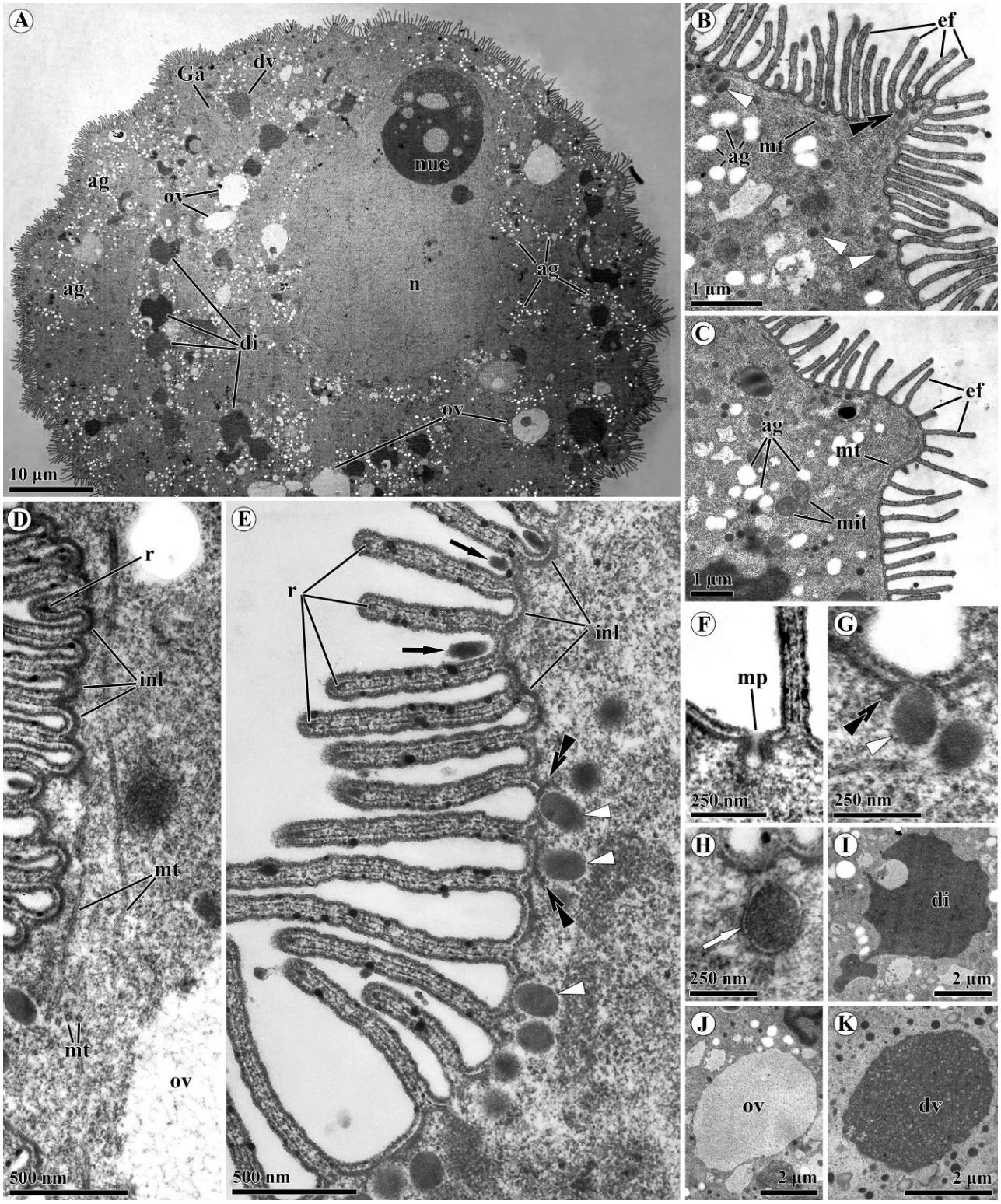

Figure 3. Fine structure of solitary *Urospora ovalis* trophozoites. **A.** Transversal section of a solitary trophozoite contracted during fixation. The nucleus (n) with the nucleolus (nuc) inside is located eccentrically in the cell. The cytoplasm is enriched by numerous and different inclusions: ag – amylopectin granules, di - electron-dense homogeneous inclusions of uncertain shape, dv – electron-dense vacuole with granular content,

General Morphology and Ultrastructure of *Urospora travisiae*

Solitary trophozoites were found in the host body cavity (Fig. 1A). Some gregarines were attached to the intestine wall (Fig. 5A) and occasionally to the blood vessels, but they easily detached during host dissection or sample manipulation. The young trophozoites and syzygies of *U. travisiae* were observed rarely during this study (Fig. 5B-C). Young trophozoites were elongated, and drop-like in shape, with up to three transverse constrictions at the tapering end. The length of them varied from 100 to 130 μm (n = 2) (Fig. 5B). The nucleus was located in the widest part of the cell. Detached young trophozoites exhibited a gliding motility, with a wide, rounded leading end.

Mature trophozoites of *U. travisiae* were V-shaped. They possessed two narrowing branches and attached to the host tissue with the tip where the branches converged, the so-called attachment tip. In syzygies, the V-shaped partners were in contact with each other by means of this attachment tip (Fig. 5C); however, the contact was not strong, and partners easily disassociated.

Each branch had 5-15 transverse permanent constrictions; thus, branches appeared as a string of pearls with differently sized beads (Fig. 5D-G). The angle between the branches in a cell varied in the range from 10° to 180°, generally from 90° to 130° (n = 25) (Figs 5D-G, 6A). Commonly, one of the branches was longer than the other: 195-660 μm (av. 392 μm; standard deviation (SD) = 99.4; n = 25) vs. 165-580 μm (av. 352 μm; SD = 96.8; n = 25). A single oval nucleus with 2-3 nucleoli was usually situated in the longest branch close to the attachment tip (Fig. 5D-G).

Detached V-shaped trophozoites demonstrated the typical gliding motility. Cells with an angle of about 10° - 100° between their branches usually moved with the attachment tip forward. The gliding path was straight or curved, as if the cell branches possessed equal or different motion forces, respectively (Supplementary Material Video 2). In cases where the angle was about 180°, cells glided with one of the branches forward.

The attachment tip appeared like a plateau, usually surrounded by a circular, wide furrow (Fig. 6B). Some traces of the epicytic folds were visible on the surface of the plateau, while the well-developed longitudinal folds extended radially from the circular furrow. Most of these aforementioned folds ran parallel till the distal end of each branch (Fig. 6A-E). On the lateral surface of the cell, the folds, passing from opposite branches, converged and merged with each other, while on the inner side of the V-shaped cell, the epicytic folds passed continuously from one branch to another (Fig. 6F). There were no evident changes in the form or structure of these folds in the region close to the attachment tip and at the constrictions between individual beads (Fig. 6E-G). Some of the folds ended at constriction regions, while others continued to the next beads. Additional epicytic folds that passed only on the surface of the beads also appeared (Fig. 6D-E).

The parasites were covered by a typical three-layered pellicle consisting of plasma membrane underlain by the closely adjacent membranes of IMC. The cortex of *U. travisiae* did not exhibit any secondary superfolds. Epicytic folds reached 0.5 μm in height and 0.1 μm in width, and were regularly distributed with a distance of about of 0.1 μm between them, 3-4 folds per 1 μm (Figs 6C, G, 7A-D). As in the epicytic folds of *U. ovalis*, the rippled dense structures and 12-nm apical filaments were indistinguishable in the apex of the epicytic fold; however, a dense fibrillar rod was observed just beneath the IMC. The pellicle was underlain

ov – electron-transparent vacuole with loose filamentous content. Ga – dictyosome of the Golgi apparatus. TEM. **B** – **C.** Details of the narrow (**B**) and wide (**C**) superfolds bearing the epicytic folds (ef). Note a micropore-like structure (black double arrowhead) and electron-dense vesicles (white arrowhead). ag – amylopectin granules, mit – mitochondria, mt – microtubules. TEM. **D.** Details of the trophozoite cortex showing peripheral transversal microtubules (mt). A single electron-dense rod (r) located just beneath the IMC is visible at the apex of one completely visible epicytic fold. inl – internal lamina, ov – electron-transparent vacuole with loose filamentous content. TEM. **E.** Transversal section of the gregarine cortex showing micropore-like structures (black double arrowhead) accompanied by electron-dense vesicles (white arrowhead). Electron-dense rods (r) are visible in the epicytic folds. Note electron-dense droplets (black arrow) between the epicytic folds. inl – internal lamina. TEM. **F.** Details of a typical micropore (mp). TEM. **G.** Details of a micropore-like structure (black double arrowhead) in contact with an electron-dense vesicle (white arrowhead). TEM. **H.** Details of an electron-dense vesicle beneath the trophozoite cortex; note the membrane (white arrow) limiting the vesicle. TEM. **I.** Higher magnification of a dense inclusion (di) of uncertain shape. TEM. **J.** Higher magnification of an electron-transparent vacuole (ov) with loose filamentous material. TEM. **K.** Higher magnification of an electron-dense vacuole (dv) with granular content. TEM.

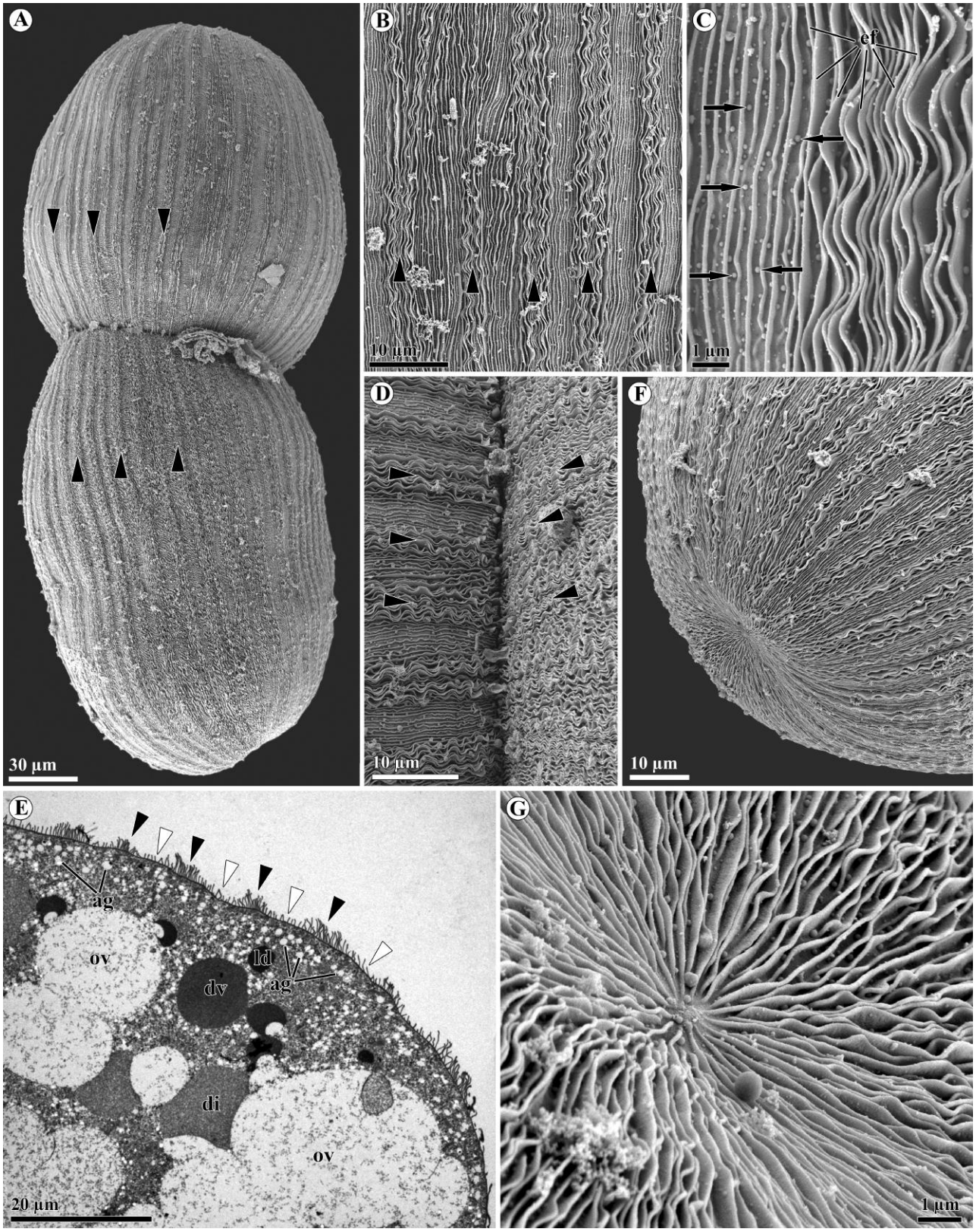
A
30 µm
B
10 µm
C
ef
1 µm
D
10 µm
F
10 µm
E
ag
ov
ld
dv
ag
di
ov
20 µm
G
1 µm

by an internal lamina, which did not form links at the base of individual epicytic folds (Fig. 7A). Typical micropores were situated between the folds (Fig. 7A). Several micropore-like structures, similar to those in *U. ovalis*, were seen between the epicytic folds. They appeared as a cone-shaped collar, formed by an IMC and internal lamina, and electron-dense vesicles were associated with them (Fig. 7B). The same vesicles were also found deeper within the parasite cytoplasm (Fig. 7D). Electron-dense inclusions, oval in profile and apparently located between the pellicle membranes, were seen at the base or at the lateral sides of most folds (Fig. 7B, D). Transversal subpellicular microtubules underlay the bases of epicytic folds, as observed in *U. ovalis* (Figs 6G, 7A).

In cross-sections of a branch near the attachment tip, the cell was almost round, and the cytoplasm was subdivided into an ectoplasm and endoplasm (Fig. 7C-E). The endoplasm was packed with electron-transparent inclusions of irregular shape, vacuoles with homogeneous translucent content, electron-dense vesicles, numerous lipid droplets, and dictyosomes of the Golgi apparatus. The ectoplasm mostly comprised mitochondria and electron-dense vesicles (Fig. 7C-E).

Molecular Phylogenetic Analysis

The new SSU sequences of *U. ovalis* (1623 bp) and *U. travisiae* (1604 bp) were obtained by direct sequencing of PCR products. There are 3.5% differences between them (46 substitutions and 3 indels) across the distance of their pairwise alignment, where they completely overlapped (1604 sites), and distinctive nucleotides did not show any polymorphism (Supplementary Material Fig. S1). Like other lecudinid and urosporid SSU rDNA sequences, the novel sequences were considerably shorter in comparison with other eukaryotes (*U. ovalis*: 1604 bp vs 1731 bp in *Bigelowiella natans* across the same interval of the alignment; *U. travisiae*: 1623 bp vs 1742 bp in *B. natans*; the full length of SSU rDNA of *B. natans* and the large majority of other eukaryotes is about 1800 bp) and contained motifs specific to other lecudinid and urosporid gregarines.

The constructed Bayesian (Fig. 8) and maximum-likelihood (ML) trees of SSU rDNA of 99 OTUs showed similar topology with two exceptions: (i) the flipped positions of two eugregarine clades: Gregarinoidea + Cephaloidophoroidea and Stylocephalids; and (ii) the branching order of archigregarines (data not shown). However, both of these variable branching patterns were weakly supported by both methods (Fig. 8).

The Bayesian tree of SSU rDNA sequences (Fig. 8) fitted recent opinions on alveolate phylogeny: the main robust clades are ciliates, dinoflagellates and apicomplexans. The backbone of the apicomplexans was weakly supported; nevertheless, the sequences clustered into several major well-supported clades: (1) coccidia and hematozoa (not supported by BP in ML analyses); (2) cryptosporidia; (3) Actinocephaloidea (Cavalier-Smith 2014) consisting of neogregarines and some terrestrial eugregarines, e.g., *Monocystis* spp. and representatives of family Actinocephalidae (not supported by BP (91%); (4) Gregarinoidea (Clopton 2009); (5) Cephaloidophoroidea (Rueckert et al. 2011a); (6) the clade of *Polyplicarium* spp. and related environmental sequences (not supported by BP (74%)); and (7) Lecudinoidea (= Urosporoidea in Cavalier-Smith 2014), a clade consisting of the marine aseptate gregarine families Lecudinidae and Urosporidae, and the unusual gregarine *Veloxidium leptosynaptae*. The SSU rDNA sequences from archigregarines did not form a common clade. All gregarine and cryptosporidia subclades formed a monophyletic clade – however, with low supports (PP = 0.81, BP = 43%), and these subclades were shuffled inside this common clade, i.e. their branching order was unresolved because of low support both in Bayesian and ML analyses. The new SSU rDNA sequences of *U. ovalis* and *U. travisiae* belonged to the Lecudinoidea clade

Figure 4. General morphology and fine structure of *Urospora ovalis* syzygies. **A**. General view of a syzygy. Black arrowheads mark sets of high epicytic folds. SEM. **B**. Detailed view of the surface showing the sets of high epicytic folds (black arrowheads). SEM. **C**. Higher magnification of the gregarine surface with low and high epicytic folds (ef). Note the droplets of mucous substance (black arrows) between folds. SEM. **D**. Detailed view of the contact between two syzygy partners. Black arrowheads indicate sets of high epicytic folds at the surface of both gamonts. SEM. **E**. Transversal section of a gamont showing the alternating sets of high (black arrowheads) and low epicytic folds (white arrowheads). Inclusions of the cytoplasm are similar to that in the cytoplasm of solitary trophozoites: ag – amylopectin granules, di – electron-dense homogeneous inclusions of uncertain shape, dv – electron-dense vacuole with granular content, ld – lipid droplets, ov – electron-opaque vacuole with loose filamentous material. TEM. **F-G**. Semi-axial view (**F**) and higher magnification (**G**) of the free ends of gamonts. Note that the apex of the free ends is slightly bulged-in. SEM.

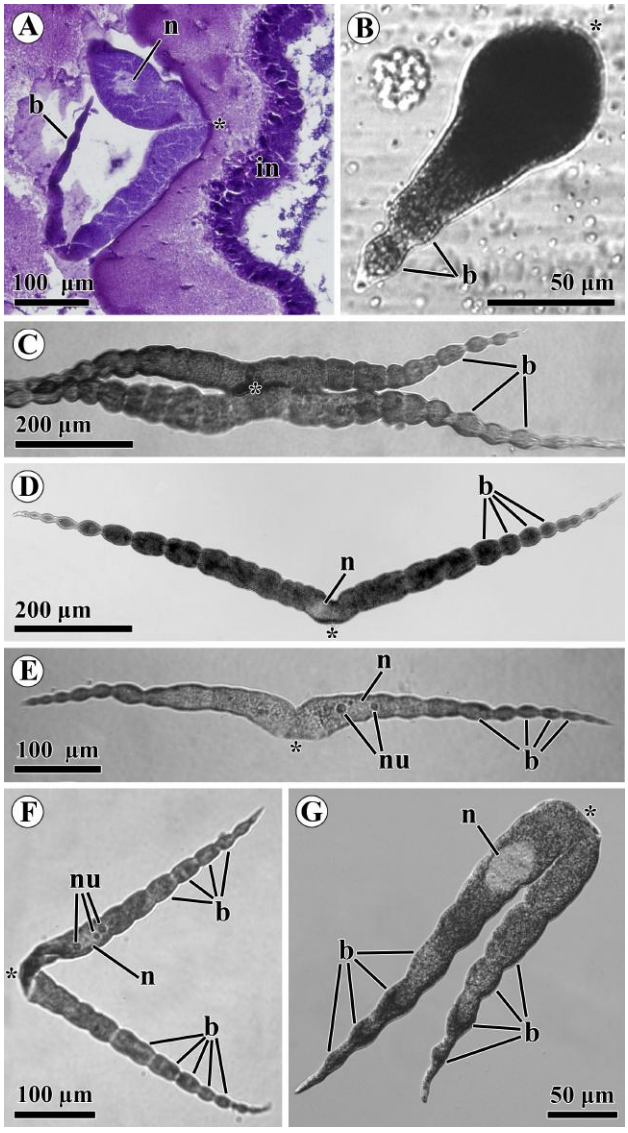

Figure 5. Light microscopic observations of *Urospora travisiae* gregarines. **A.** Histological section of the trophozoite clamped between the folds of the host intestine (in). Asterisk indicates the attachment tip, n – nucleus, b – bead of the branch in the cell. LM, H&E. **B.** Young trophozoite with a single tapering branch bearing two transverse constriction near the end. Asterisk marks the attachment tip, b – beads of the branch in the cell. BF. **C.** Syzygy of two V-shaped partners attached to each other by their attachment tips (asterisk). b – beads of the branches. BF. **D** – **G.** Micrographs of trophozoites with different angles between their branches: **D** – approx. 140°; **E** – 180°; **F** – 70°; **G** – 10°. Note the different number of the beads (b) in their branches and the oval nucleus (n) with 2-3 nucleoli (nu) situated in the longest branch close to the attachment tip (asterisk) of each individual.

(Fig. 8). Within this clade, however, they closely affiliated with lecudinids (*Difficilina* species), but not with other urosporids (*Pterospora* spp. and *Lithocystis* spp.).

Despite the fact that the new sequences were fully supported by both the BI and ML analyses in the 99 OTUs tree, topological tests were performed using the resulting phylogeny of 23 selected lecudinid and urosporid sequences (Fig. 9A-I, Table 2). The topology of the main clades in this tree (Fig. 9A) remained the same as the topology of those in the 99 OTUs tree. Further, 8 trees with alternative topologies were constructed (Fig. 9B-I), in which the clade *U. ovalis* + *U. travisiae* sequentially changed their position. We tested all of these topologies using a set of the most common tests. The majority of topologies were discarded with the exception of three permissible ones: the Bayesian tree, the alternative topology F (but not the BP test), and the alternative topology I (Fig. 9A, F, I, Table 2). All these trees contained the clade *Difficilina* spp. + *Urospora* spp. in contrast to the discarded topologies, where this combination was absent.

Discussion

The morphology of the gregarines investigated in this study completely corresponds to the original description of *Urospora ovalis* and *U. travisiae* trophozoites presented by V. A. Dogiel (1910). According to the original descriptions, oocysts of *U. ovalis* and *U. travisiae* were heteropolar (with a funnel and a tail at opposite ends), very similar, but differ in size; oocysts of *U. travisiae* were larger than those of *U. ovalis* (Dogiel 1910). All oocysts observed in the present study were of the same size and typical of representatives of the genus *Urospora*. Although, species affiliation of the observed oocysts was not identified in this study, they obviously belong to one of the investigated species.

The investigated gregarines differ in cell shape and morphology (Table 1). In *U. ovalis*, the solitary trophozoites do not demonstrate any signs of cell heteropolarity. This phenomenon was also described for gamonts of *Gonospora ormieri* (Porchet 1978). Young and mature trophozoites of *U. travisiae* are heteropolar. The young individuals of *U. travisiae* can attach to the substrate with the wider end, which is most likely the anterior end. We assume that during gregarine growth, a second branch of the cell starts to develop, so that the cell gradually transforms from a monoaxial to a V-like biaxial form. The anterior end of the

Table 2. Results of alternative topology tree tests (alignment of 23 OTUs, 1676 bp).

Tree topology	– ln L	BP[a]	ELW[b]	KH[c]	SH[d]	WSH[e]	AU[f]
Bayesian consensus tree (Fig. 9, A)	**13536.74**	**0.84736**	**0.84736**	**1.0**	**1.0**	**1.0**	**0.9023058**
Alternative topologies							
B	13686.58	0	0	0	0	0	0
C	13747.51	0	0	0	0	0	0
D	13813.34	0	0	0	0	0	0
E	13813.32	0	0	0	0	0	0
F	**13541.49**	0.04601	**0.07659232**	**0.11657**	**0.64057**	**0.37045**	**0.1236613**
G	13698.65	0	0	0	0	0	0
H	13747.51	0	0	0	0	0	0
I	**13541.15**	**0.10663**	**0.1215358**	**0.13904**	**0.65436**	**0.41608**	**0.1578981**

[a]Bootstrap Probability (Felsenstein 1985);
[b]Expected-Likelihood Weights (Strimmer and Rambaut 2002);
[c]P-value of the Kishino-Hasegawa test (Kishino and Hasegawa 1989);
[d]P-value of the Shimodaira-Hasegawa test (Shimodaira and Hasegawa 1999);
[e]P-value of the Weighted Shimodaira-Hasegawa Test (Shimodaira and Hasegawa 1999);
[f]P-value of the Approximately Unbiased test (Shimodaira 2002). P-values <0.05 discard the suggested topology. Permissible topologies are bolded.

young cell remains as the attachment site of V-like shaped cell. The older (or primary) branch is usually longer and contains the nucleus. It is important to note that trophozoites of *Pterospora* spp. can be characterised as biaxial as well (Dogiel 1910; Landers 1991, 2001; Landers and Gunderson 1986; Leander 2008).

Most eugregarines possess a cortex with a complicated structure (Schrével et al. 1983; Vivier 1968; Vivier et al. 1970). Investigated gregarines from *Travisia forbesii* also possessed a well-developed cortex with numerous longitudinal epicytic folds. In both species, rippled dense structures (RDS) and 12-nm apical filaments were not well preserved and were poorly detectable only in a few folds, despite the application of different fixation protocols. Electron-dense rods, observed in both species, were located in the apex of the longitudinal folds, under the IMC, and appear to be similar to those described in *Gonospora beloneides, Lankesteria* spp., *Gregarina* spp., *Difficilina cerebratuli*, *Thiriotia pisae*, *Ganymedes vibiliae*, and *Porospora portunidarum* (Corbel et al. 1979; Desportes et al. 1977; Simdyanov 1995a, 2009; Valigurová et al. 2013). It was assumed that it has the role of reinforcing the fold tips (Valigurová et al. 2013).

Micropores, appearing as invaginations of the plasma membrane encircled by a collar formed from the IMC, are typical for apicomplexans. The exact function of these structures, although often discussed, remains unclear. Micropores could function as organelles for the acquisition of nutrients (Chobotar and Scholtyseck 1982; Scholtyseck 1973; Scholtyseck and Mehlhorn 1970; Vivier et al. 1970) or as extrusomes for mucus secretion (Desportes and Schrével, 2013; Philippe and Schrével 1982; Valigurová et al. 2013; Vegni Talluri and Dallai 1983). We observed typical micropores and micropore-like structures (MLS) in *U. ovalis* and *U. travisiae*. We assume that typical micropores play a role in the gregarine's acquisition of nutrients, while the second structures serve to secrete mucus onto the parasite surface in between the folds. Under SEM and TEM, the excreted mucus appears as droplets (Fig. 3E, 4B), as was also demonstrated in other gregarines (Simdyanov 1995a, 2009; Valigurová et al. 2013; Walker et al. 1984). In addition, the pore-like structures interrupting the IMC (and the plasma membrane, in some cases), but lacking the collar, were documented in the attachment site at the top of the protomerite of *Gregarina cuneata* gamonts (Valigurová 2012). These structures could also play a role in the secretion of adhesive material, which is often present between the attached gregarine and adjacent host tissue. Mucous material was also observed on the sucker-like protomerite of some actinocephalid eugregarines (Cook et al. 2001).

In a series of transverse sections of the studied gregarines, we observed the non-uniform accumulation of presumably mucus-secretory vesicles under the pellicle. It allows us to speculate that mucus excretion occurs with different intensities

in various zones of the parasite surface at the same moment. Therefore, an eruptive (or impulsive) nature of the mucus excretion could take place in the investigated gregarines. We can assume that the release of the mucus by gregarine into the environment may serve as a protective mechanism against attack by host coelomocytes. It is expected that the gliding motility of eugregarines is facilitated by the specific structure of the epicytic folds; therefore, mucus secretion may also help to decrease frictional forces during forward movement. This was previously proposed for *Gregarina* spp., in which the mucus load in the gregarine cytoplasm was positively correlated with gliding speed (King 1981, 1988; Mackenzie and Walker 1983; Valigurová et al., 2013; Vávra and Small 1969).

Gliding motility is characteristic of the majority of eugregarines. This motility can easily be observed in free (non-attached) eugregarines contacting with a substrate, when they move forward, usually without any obvious changes in their cell shape (unlike metaboly or rolling). However, when attached to the host tissue, eugregarines do not usually demonstrate any signs of motility, although near-surface currents in the internal environment of the host can be noticed around parasites. Obviously, parasites produce these currents by themselves. It is important to note that contact between a gregarine and solid matter might not be necessary for gregarine motion, as *Gregarina* spp. gamonts are able to free-float in a liquid lacking any contact with the substrate and with a significantly higher rate than exhibited during regular gliding (Valigurová et al. 2013).

Metaboly is another type of motility, which is accompanied by significant changes in cell shape. Gregarines demonstrating metabolic (or peristaltic) motility, or even immobility, as a rule, possess an epicyte of unusual organisation. Various modifications of the epicyte typical for eugregarines along with the loss of gliding motility have been reported in representatives of the families Monocystidae and Urosporidae, parasitising the coelom, respiratory trees, and seminal vesicles of various invertebrates (Dyakin and Simdyanov 2005; Frolov 1991; Landers 1991, 2001; Landers and Gunderson 1986; Landers and Leander 2005; MacMillan 1973; Miles 1968; Vinckier 1969; Vinckier and Vivier 1968). *Urospora ovalis* and *U. travisiae* both possess a typical epicyte; nevertheless, the trophozoites and young syzygies of *U. ovalis* demonstrate metabolic motility, during which the cell cortex in the contracted regions generates several superfolds. Similar superfolds have been documented in trophozoites of *Nematocystis magna*, a monocystid eugregarine demonstrating peristaltic-like motility (MacMillan 1973; Miles 1968). Mitochondria observed in *U. ovalis* are similar to those reported in *Pterospora floridensis* (Landers 2002). We assume that the relatively great number of mitochondria distributed uniformly in the cell cytoplasm appears to be correlated with the active metaboly of *U. ovalis.*

The motility of gregarines seems to be an adaptation to their localisation in a certain niche in the host body. Gregarines inhabiting the host digestive tract usually possess pendular or gliding motility types (e.g. *Selenidium* spp., *Lecudina* spp.). They develop clamped in narrow spaces between the intestinal folds or between the intestine and food. We assume that motility in intestinal gregarines might be necessary to provoke an exchange of host internal environmental liquids around them in order to improve the effectiveness of their nutrient acquisition and/or reduce frictional forces to retain the attachment to host tissues, as also suggested by Leander (2008). This also applies to *U. travisiae*, which attaches to the outer wall of the intestine. Metaboly seems to be characteristic of detached parasites (numerous representatives of the families Urosporidae and Monocystidae) inhabiting the host body cavities. Presumably, monocystids have acquired this type of motility as an adaptation to their life style, being detached and motile within the gametes agglomeration of oligochaete hosts. Moreover, some urosporids could have evolved their motility as an adaptation for living in the liquid environments of host cavities without any attachment to host tissue. In addition, motility in gregarines could provide an effective protection against the adhesion of host coelomocytes to their surfaces, as shown for other coelomic parasites (De Ridder and Jangoux 1984; Coulon and Jangoux 1988, 1991; Siedlecki 1903).

Both gregarines investigated in this study showed signs of active metabolism, represented by the presence of various vacuoles and inclusions. We assume that, along with an increase in amylopectin load, the maturation of trophozoites of both species is accompanied by an increase in the quantity and size of these inclusions and vacuoles, which occupy almost the entire cell volume. Their function remains unclear; however, we can suggest that their contents may be used for further gametocyst and oocyst wall formation, similar to wall-forming bodies in coccidia (Long 1982).

The frontal and lateral syzygies are characteristic of urosporids (Levine 1977). In the present study, we documented end-to-end syzygy in *U. ovalis* and frontal syzygy in *U. travisiae*. We cannot identify the exact type of syzygy present in *U. ovalis* gregarines:

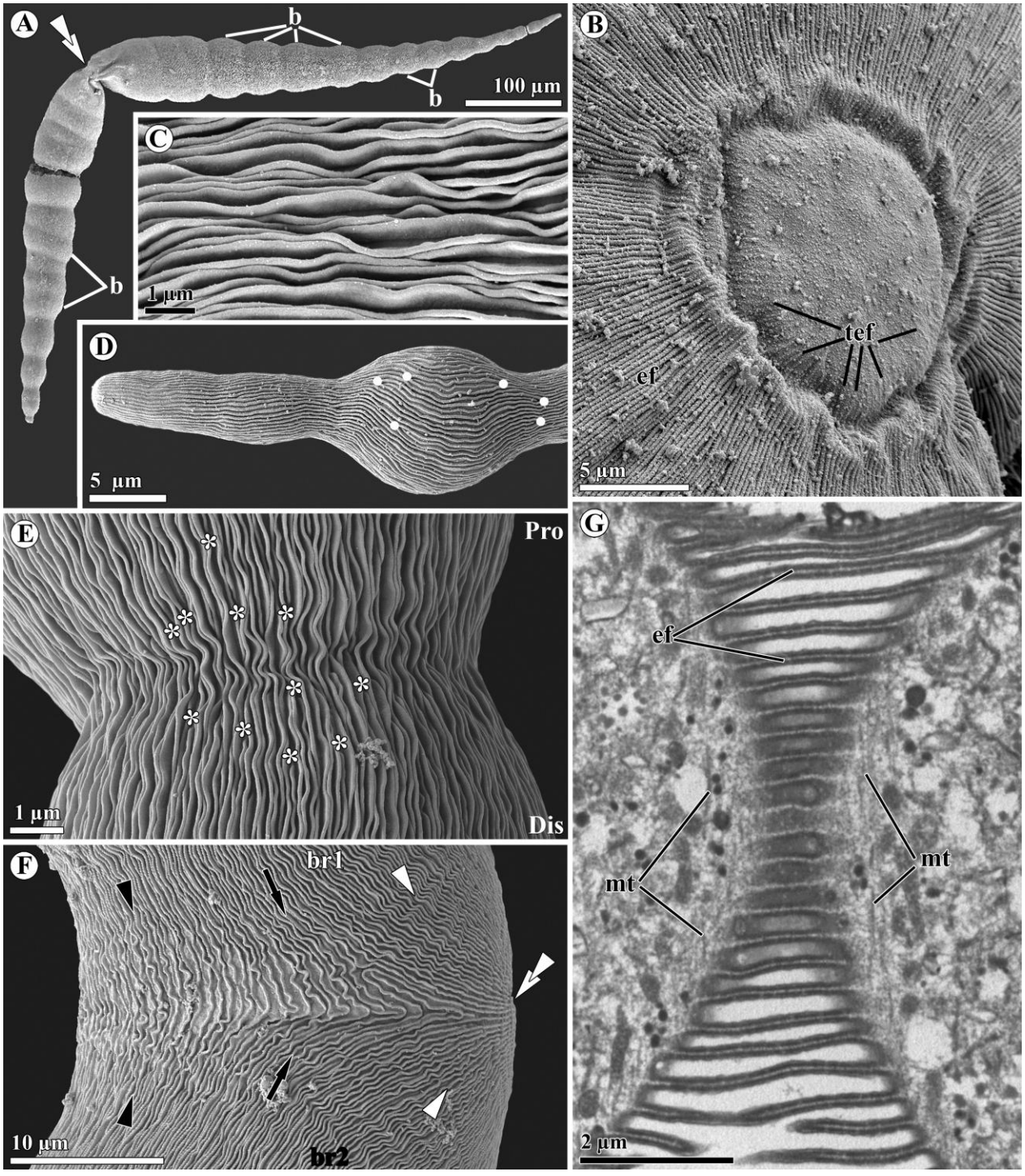

Figure 6. General morphology and fine structure of *Urospora travisiae* trophozoites. **A**. General view of a trophozoite. White double arrowhead points to the attachment site placement, b - beads of the branches. SEM. **B**. Detailed view of the attachment tip; traces of the epicytic folds on the surface of the plateau (tef) and well-developed epicytic folds (ef) extended from the furrow are well visible. SEM. **C**. Higher magnification of the gregarine surface demonstrating epicytic folds. SEM. **D**. Higher magnification of the distal part of the branch with one bead. White dots mark the beginning/end of additional epicytic folds on the bead surface. SEM. **E**. Higher magnification of the constricted region between two individual beads. Asterisks mark the epicytic folds terminating near the region of constriction. Dis – distal end of the branch, Pro – proximal end of the branch.

caudo-frontal, frontal, or caudal. The syzygy of *U. travisiae* is obviously frontal, as partners are in contact by their attachment tips. Syzygies of *U. travisiae* are comparable with those of *Pterospora* spp., in which partners are of V-like shape, with two piriform branches possessing posterior dendritic trunks (Landers 1991, 2001; Landers and Gunderson 1986; Landers and Leander 2005).

Molecular phylogenetic analyses confirmed the morphological data: both species belong to the clade Lecudinoidea comprising representatives of the families Lecudinidae and Urosporidae. Previously, it was shown that, within the Lecudinoidea clade, some species have small interspecific differences (Mita et al. 2012; Rueckert et al. 2015). Alternatively, some of them have high intraspecific differences in SSU rDNA (Rueckert et al. 2011b), even in the species with negligible morphological interspecific differences (Rueckert et al. 2010). In a pair of studied species *U. ovalis* and *U. travisiae* a set of distinctive sites in the sequences was identified by direct sequencing of PCR products from genomic DNA obtained from 10-20 individuals of each species, and distinctive nucleotides were neither polymorphic nor ambiguous (Supplementary Material Fig. S1). Consequently, there is a genetic hiatus conforming to considerable morphological differences between gregarines of these species. Further investigations including single-cell sequencing and analysing of other genetic markers, such as ITS2, LSU rDNA and the whole ribosomal operon sequences, are desirable for revealing of distinctions, undiscovered by cell-pool sequencing, between *U. ovalis* and *U. travisiae*.

In our study, the representatives of the families Lecudinidae and Urosporidae were partially mixed with each other (clades corresponding to these families were not well-supported). At the same time, representatives of the family Urosporidae exhibited a clear diagnostic feature, probably a synapomorphy: the characteristic morphology of oocysts, with a funnel at one of the poles and one or more projections of the oocyst wall, sometimes quite long, at the opposite pole (Dogiel 1906, 1909, 1910; Léger 1892). Therefore, we assume that SSU rDNA phylogeny cannot resolve the real branching order in the clade Lecudinoidea, either because of the insufficient sensitivity of the method or because of the limited number of taxon samples. Furthermore, removing the *Veloxidium leptosynaptae* sequence (see below) from the analysis led to the uniform shuffling of all lecudinids and urosporids within the clade (data not shown). The high sensibility of gregarine SSU rDNA phylogeny to taxonomic sample size was noted earlier (Simdyanov et al. 2015). On the other hand, SSU rDNA phylogeny confirms the close relations between lecudinids and urosporids, which were included in the 'aseptate' eugregarines, parasites of marine invertebrates, according to Grassé's concept of host-parasite coevolution (Grassé 1953).

In this study, *Veloxidium leptosynaptae*, an unusual gregarine from the intestine of the sea cucumber *Leptosynapta clarcki*, was closely affiliated with the clade Lecudinoidea (Figs 8, 9). In addition, the SSU rDNA sequence of *V. leptosynaptae* possessed motifs that were unique to this clade. However, on the basis of the bending motility and surface morphological characteristics of the gregarine, the authors of the original description of *V. leptosynaptae* (Wakeman and Leander 2012) suggested that this species belongs to the order Archigregarinorida. Nevertheless, they noticed that the 'Veloxidium clade' branched as the nearest sister lineage to the clade of marine lecudinids and urosporids. We have several objections to such a classification of *V. leptosynaptae*: 1) the syzygy of *V. leptosynaptae* appears frontal (typical for lecudinids) rather than caudal (typical for archigregarines); and 2) some eugregarines are also capable of bending their body, sometimes quite dramatically (Hildebrand 1981; Simdyanov, 1995b; Valigurová et al. 2013). Therefore, further TEM studies of the cortex are necessary to establish the taxonomic position of *V. leptosynaptae* more reliably.

It was suggested that coelomic gregarines evolved more than once from different marine intestinal eugregarines (Leander et al. 2006). One of the possible ways for the transition from intestinal to coelomic parasitism was demonstrated in some marine eugregarines from polychaetes when, during host reproductive metamorphosis, intestinal gregarines located in the host body cavity for a short time (Durchon and Vivier 1961). Such temporary location of gregarines in the host coelom

SEM. **F**. Higher magnification showing converging and merging epicytic folds (black arrows) that cover the lateral side, black arrowheads mark folds passing from one branch (br1) to another (br2) on the inner surface of the cell near the attachment tip, and folds (white arrowheads) arising from the attachment tip (white double arrowheads). SEM. **G**. Tangential section of the constricted region between adjoining beads. ef – epicytic folds; mt – microtubules. TEM.

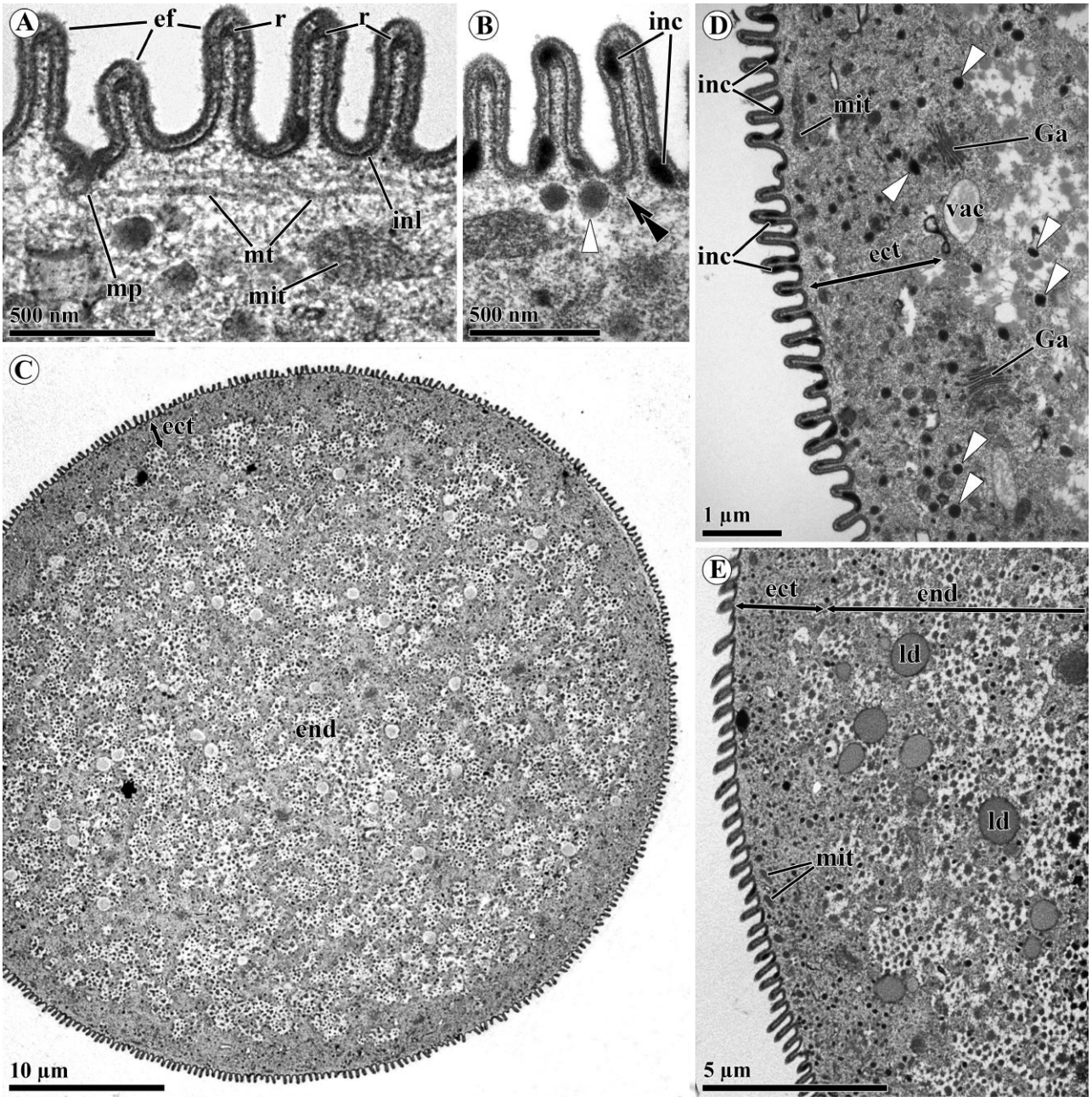

Figure 7. Fine structure of the cortex and cytoplasm of *Urospora travisiae* trophozoites. **A**. Transversal section of a trophozoite demonstrating the cell cortex in detail. Note a typical micropore (mp) between epicytic folds (ef) and an electron-dense rod (r) in the apex of each fold. inl – internal lamina, mit – mitochondrion, mt – microtubules. TEM. **B**. Transversal section of the gregarine cortex showing a micropore-like structure (black double arrowhead) with a closely located electron-dense vesicle (white arrowhead), and an electron-dense inclusion between cortex cytomembranes (inc). TEM. **C**. Transversal section of one of the branches near the attachment tip. The cytoplasm is subdivided into ectoplasm (ect) and endoplasm (end). TEM. **D.** Transversal section of a trophozoite demonstrating the cell cortex and ectoplasm (ect) in detail. Ga – Golgi apparatus, inc – electron-dense inclusion; mit – mitochondrion, vac – electron-transparent vacuoles. TEM. **E**. Detailed view of the cell ecto- (ect) and endoplasm (end) in transversal section; ld – lipid droplets; mit – mitochondrion. TEM.

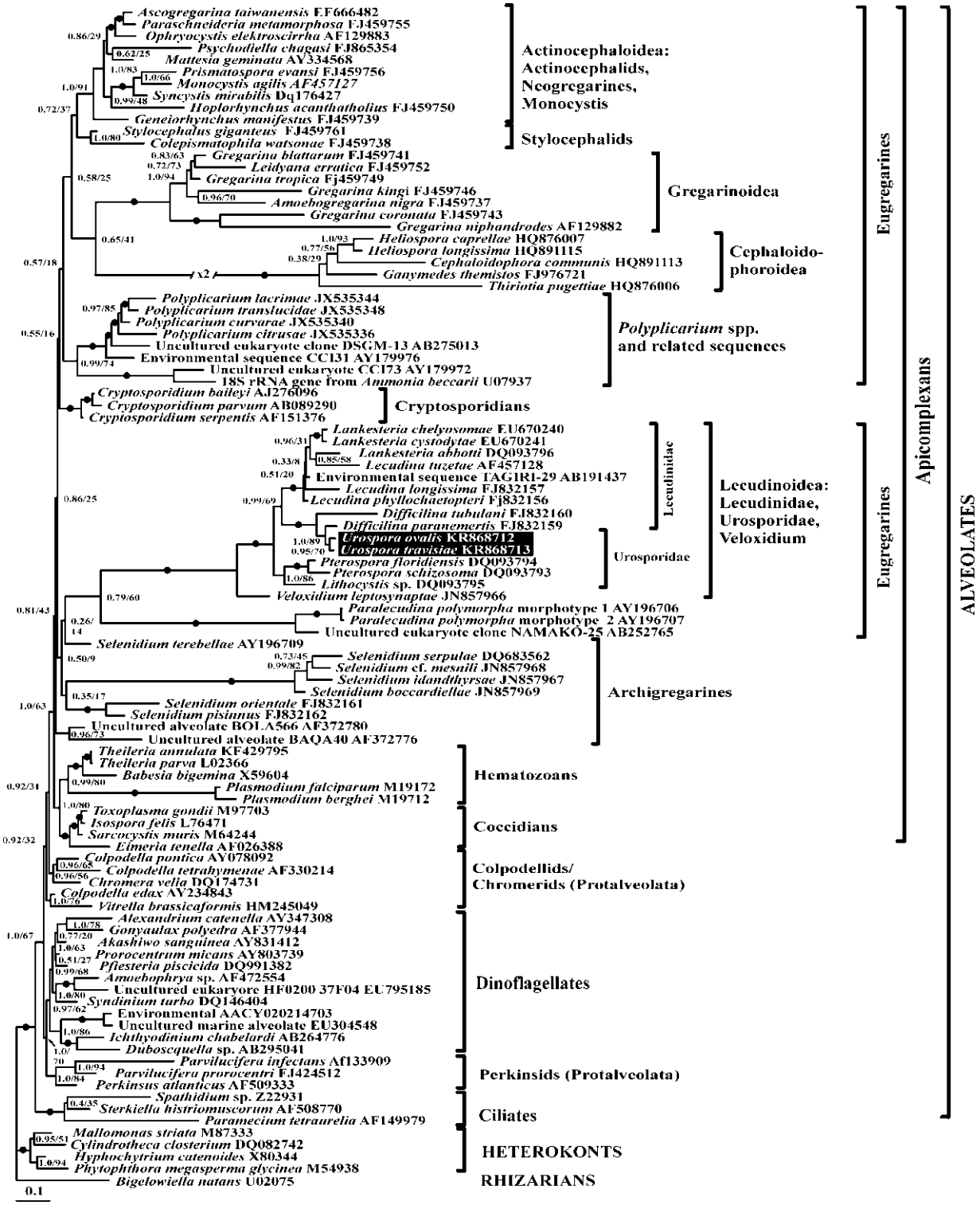

Figure 8. SSU rDNA Bayesian tree of alveolates (99 OTUs, alignment of 1557 bp) constructed using the GTR+Γ+I model. Numbers at the nodes denote Bayesian posterior probabilities (numerator) and ML bootstrap percentage (denominator). Black disks on the branches indicate the Bayesian posterior probabilities and the bootstrap percentages equal to or more than 0.95 and 95%, respectively. A black box highlights the sequences from *Urospora ovalis* and *U. travisiae*.

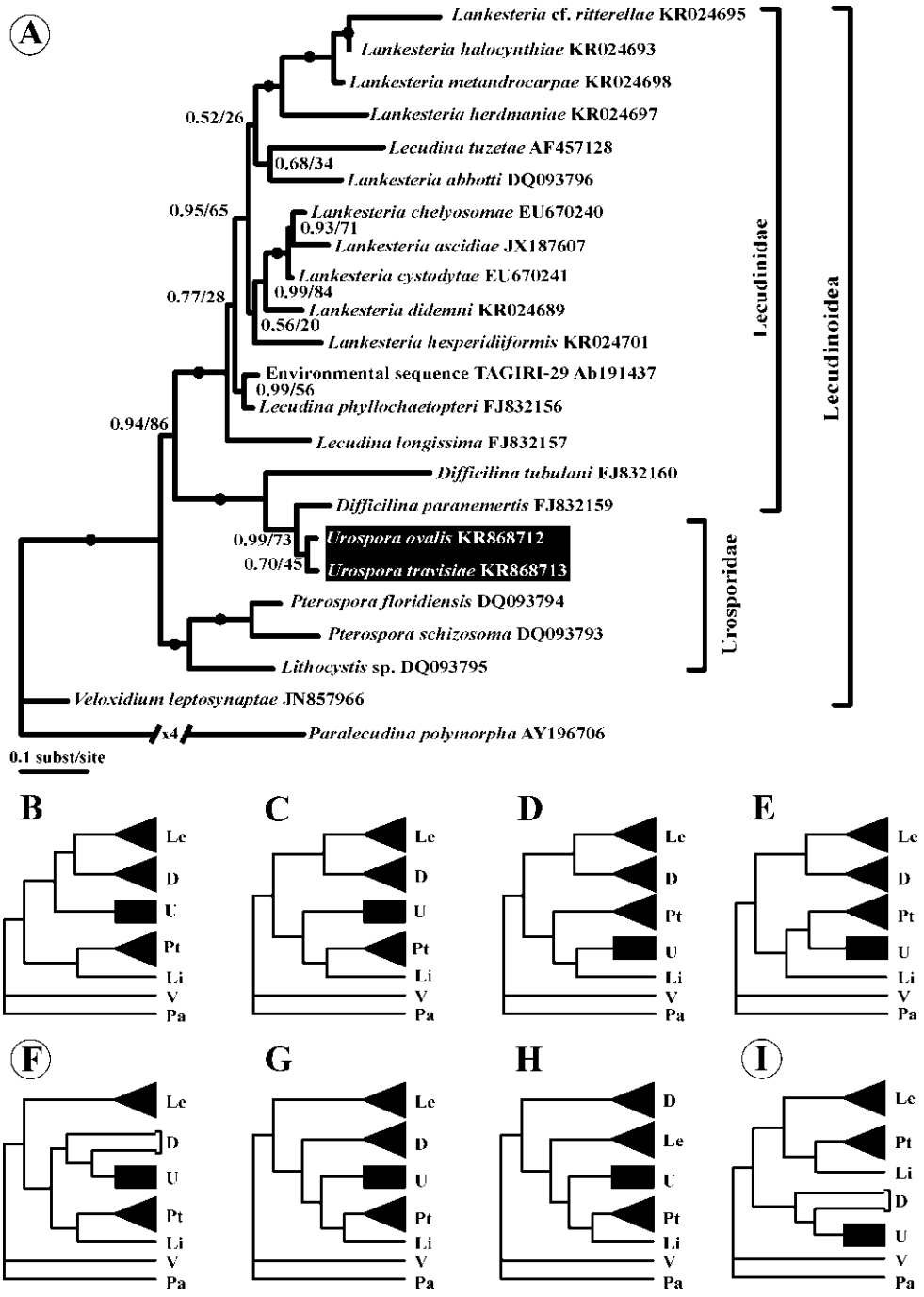

Figure 9. Results of topology tests of 23 selected lecudinid and urosporid sequences. **A**. SSU rDNA Bayesian tree of selected OTUs (alignment of 1676 bp) constructed using the GTR+Γ+I model (8 categories). Numbers at the nodes denote Bayesian posterior probabilities (numerator) and ML bootstrap percentage (denominator). A black box highlights the sequences from *Urospora ovalis* and *U. travisiae*; black disks on the branches indicate the Bayesian posterior probabilities and the bootstrap percentages equal to or more than 0.95 and 95%, respectively. **B** – **I**. alternative topologies which were tested together with tree A; there are just three permissible topologies: **A**, **F**, and **I,** marked by circles. Abbreviations: D = *Difficilina* spp., Le = *Lecudina* spp. + *Lankesteria* spp., Li = *Lithocystis* sp., Pa = *Paralecudina polymorpha*, Pt = *Pterospora* spp., U = *Urospora* spp., V = *Veloxidium leptosynaptae*.

could be fixed in their life cycle. It is an argument that supports the hypothesis that haemocoelic gregarines originated from intestinal ones in insects (Léger 1892). The explanation for such a transition is that phylogenetically related parasites, occupying different ecological niches in the host, decrease the intensity of species competition, and demonstrate diverse adaptations to parasitism (Wakeman et al. 2014).

Conclusions

This study revealed that the closely related eugregarines *Urospora ovalis* and *U. travisiae*, inhabiting the coelom of the polychaete *Travisia forbesii*, demonstrate different strategies of parasitism. The V-shaped cells of *U. travisiae* attach to the host and retain gliding motility when detached. In contrast, the cells of *U. ovalis* are oval-shaped, non-attached, and exhibit peristaltic activity. Both gregarines possess a typical organised cortex with epicytic folds of similar structure. In metabolic *U. ovalis*, the cell cortex generates superfolds in the contracted regions.

Methods

The cells of both gregarine species (*Urospora ovalis* and *Urospora travisiae*) were isolated from the coelom of the marine polychaete *Travisia forbesii* Johnston, 1840. The hosts were collected from June to July each year from 2004 to 2006 and in the second half of August each year from 2011 to 2013 at upper sublittoral of two sites: in the vicinity of the Marine Biological Station of Saint-Petersburg State University (inlet Yakovleva, Chupa Inlet, Kandalaksha Bay, White Sea, 66°18′99″N, 33°49′95″E) and the White Sea Biological Station of Moscow State University (Rugozerskaya Inlet, Kandalaksha Bay, White Sea, 66°33′12″N, 33°06′17″E).

The dissection of hosts and subsequent manipulation with parasites was performed under MBS-10 stereomicroscopes (LOMO, Russia). Light micrographs were provided using an MBR-1 microscope (LOMO, Russia) equipped with phase contrast and connected to a Canon EOS 300D digital camera. The gregarines of both species were isolated separately with thin glass pipettes, washed in Millipore filtered sea water (SW) (Millex-GC 0.22 μm) and subsequently prepared for light, electron microscopy and DNA extraction.

Histological procedure: Several entire worms were anesthetised and fixed in AFA (Alcohol–Formalin–Acetic Acid) fixative solution. The material was dehydrated through a graded alcohol series, cleared in xylene, infiltrated in a graded series of xylene/Histoplast II (3:1, 1:1, 1:3) and finally embedded in Histoplast II (Sigma-Aldrich, Czech Republic). Serial sections (transversal, sagittal, and coronal) of the fixed worms were prepared on a Microm HM 360 rotary microtome and stained with haematoxylin-eosin. Micrographs were obtained using an Olympus BX61 microscope equipped with an Olympus DP 71 digital camera.

Electron microscopy: The hosts were dissected and the parasites were collected separately from the host body cavity using thin glass pipettes. The trophozoites were fixed in 2% or 2.5% glutaraldehyde in 0.1 M cacodylate buffer (CB), 0.1 M PBS, or SW. For transmission electron microscopy the gregarines were then post-fixed with 1% OsO_4 (Os) in 0.2 M CB, 0.1 M PBS or SW, dehydrated in an ethanol series, and embedded into Epon blocks. The ultra-thin sections were stained according to standard protocols (Reynolds 1963) and observed with LEO-910 and JEOL-1010 transmission electron microscopes. For scanning electron microscopy, fixed trophozoites were critical point dried in liquid CO_2 and then coated with gold. The samples were observed with a JEOL JSM-7401F scanning electron microscope.

DNA isolation, PCR and sequencing: Individual trophozoites of each species, about 10 and 20 trophozoites of *Urospora ovalis* and *Urospora travisiae*, respectively, were isolated from dissected hosts, washed three times in Millipore filtered SW, and deposited into 0.5 ml microcentrifuge tubes. All samples were fixed and stored in RNA-later reagent (Life Technologies, USA). DNA extraction was performed with the Diatom DNA Prep 200 kit (Isogen, Russia).

The new partial SSU rDNA sequences (1623 bp for *U. travisiae* and 1603 bp for *U. ovalis*) were amplified with Encyclo PCR kit (Evrogen, Russia) using a T3000 Thermocycler (Biometra, Germany) according to the following protocol: initial denaturation at 95 °C for 3 min; 40 cycles of 95 °C for 30 sec, 45 °C for 30 sec, and 72 °C for 1.5 min; and a final extension at 72 °C for 10 min with primers 5′-GTAGTCATAYGCTTGTCTYGC-3′ (forward) and 5′- GATCCTTCTGCAGGTTCACCTAC -3′ (reverse). Only weak bands of an expected size were obtained by electrophoresis in agarose gel; therefore, small pieces of the gel were sampled from those bands (using pipette tips under a transilluminator) and re-amplification PCR with ColoredTaq DNA polymerase kit (Silex, Russia) using the DNA Engine Dyad thermocycler (Bio-Rad) and the same primers was performed.

PCR products of the expected size were gel isolated using a Cytokine DNA isolation kit (Cytokine, Russia) and sequenced using an ABI PRISM BigDye Terminator v. 3.1 reagent kit on an Applied Biosystems 3730 DNA Analyzer automatic sequencer. The newly obtained SSU rDNA sequences (GenBank Accession numbers: *Urospora ovalis* KR868712 and *Urospora travisiae* KR868713) were preliminarily identified by BLAST analysis including the built-in NJ-tree tool.

Molecular phylogenetic analysis: The two novel SSU rDNA sequences were aligned with 97 other SSU rDNA sequences, representing the major lineages of apicomplexans, as well as dinoflagellates, ciliates, heterokonts and rhizarians as outgroups, using the MUSCLE 3.6 programme (Edgar 2004) and manual tuning with the BioEdit 7.0.9.0 programme (Hall 1999). After removing hypervariable regions, the length of the alignment of the final 99 operational taxonomic units (OTUs) was 1557 sites. Bayesian analysis of this alignment was conducted using the MrBayes 3.2.1 programme (Ronquist and Huelsenbeck 2003). The programme was set to operate using the following parameters: nst = 6, ngammacat = 8, rates = invgamma, covarion = yes; parameters of Metropolis Coupling Markov Chains Monte Carlo (mcmc): nchains = 4, nruns = 4, temp=0.2, ngen = 7 000 000, samplefreq = 1 000, burninfrac = 0.5 (the first 50% of 7 000 sampled trees, i.e. the first 3500, were discarded in each run). An average standard deviation of split frequencies of 0.013232 was achieved at the end of calculations. Maximum-likelihood analysis of the 99 OTU alignment and calculations of Bayesian tree bootstrap support were performed with the RAxML 7.2.8 programme (Stamatakis 2006) under the GTR+Γ+I model with 4 categories of discrete gamma

distribution. The procedure included bootstrap analysis with 1000 replicates and 100 independent runs of ML analysis. All of these computations were performed using the University of Oslo Bioportal free service (www.bioportal.uio.no).

For the testing of alternative topologies, another alignment of 23 selected OTUs including lecudinids and urosporids (all available sequences from GenBank) was created. The sequences of *Veloxidium leptosynaptae* and *Paralecudina polymorpha* were used as outgroups for this analysis. This gave us the opportunity to include 119 additional nucleotides from hypervariable regions in the analyses, so that the final length of the alignment increased to 1676 bp. Topology tests for the 23 OTUs Bayesian tree were performed using the TREEFINDER programme under the same model as in the Bayesian analyses (GTR+Γ+I, 8 categories) (Jobb 2011; Jobb et al. 2004).

List of Abbreviations

BF – Bright Field light microscopy; CB – Cacodylate Buffer; DIC – Differential Interference Contrast microscopy; IMC – Inner Membrane Complex; H&E – Haematoxylin & Eosin staining; LM – Light Microscopy; ML – Maximum-likelihood analyses; MLS – Micropore-like structures; OTU – Operational Taxonomic Unit; PBS – Phosphate Buffered Saline; PC – Phase Contrast light microscopy; RDS – Rippled Dense Structure; SEM – Scanning Electron Microscopy; SW – Sea Water; TEM – Transmission Electron Microscopy

Author Contributions

AD and GGP conceived and designed the study, performed field sampling, carried out the research, performed the light and electron microscopic analyses, and wrote the manuscript. AD and TGS designed and performed the molecular-biology experiments and phylogenetic analyses. VVA provided the laboratory equipment, necessary reagents, and materials, and gave consultations. AV contributed to material collection and processing (2011-2013), to the light microscopic observations, and to the interpretation of microscopic data. All authors contributed to the writing of the manuscript, and read and approved the final manuscript.

Acknowledgements

The authors are grateful to the staff of the Marine Biological Station of Saint-Petersburg State University (MBS SPbSU) and the Nikolai Pertsov White Sea Biological Station of Lomonosov Moscow State University (WSBS MSU) for providing them with on-site facilities for field sampling and material processing. The authors are greatly indebted to members of the Laboratory of Electron Microscopy (Institute of Parasitology, BC ASCR in České Budějovice) for their technical assistance. AD and GGP would like to thank Andrej Dobrovolskij (Dept. of Invertebrate Zoology, St. Petersburg State University) for initiating this study, and also Vladimir Semenov and Tatiana Kharkievitch (Sechenov Institute of Evolutionary Physiology and Biochemistry of the Russian Academy of Sciences) for their assistance with electron microscopy. A part of the present study was performed at the Resource Centres (Culture Collections of Microorganisms, Molecular and Cell Technologies, Observatory of Environmental Safety) of St. Petersburg State University. GGP is grateful to Professor Rudolf Entzeroth for providing facilities for her research at Dresden Technical University (TUD) and to Markus Gunther (TUD) for his assistance with SEM. DNA sequencing was performed at the “Genome” DNA sequencing centre (Engelhardt Institute of Molecular Biology, Russian Academy of Sciences, www.genome-centre.ru). AV and AD were funded by project No. GBP505/12/G112 from the Czech Science Foundation (ECIP - Centre of Excellence) and acknowledge support from the Department of Botany and Zoology, Faculty of Science, Masaryk University towards the preparation of this manuscript. GGP was supported by St. Petersburg State University grants (1.42.1493.2015, 1.42.1099.2016), a Michail Lomonosov stipendium (DAAD), and TUD grants. TGS was supported by grants from the Council of the President of the Russian Federation (NSh-7770.2016.4) and from the Russian Foundation of Basic Research (15-29-02601). The phylogenetic analysis in this study was supported by Russian Scientific Foundation grant No. 14-50-00029. The authors also grateful to Matthew Nicholls for English proof-reading.

Appendix A. Supplementary data

Supplementary data associated with this article can be found, in the online version, at http://dx.doi.org/10.1016/j.protis.2016.05.001.

References

Adl SM, Simpson AG, Lane CE, Lukes J, Bass D, et al. (2012) The revised classification of eukaryotes. J Eukaryot Microbiol **59**:429–493

Cavalier-Smith T (2014) Gregarine site-heterogeneous 18S rDNA trees, revision of gregarine higher classification, and

the evolutionary diversification of Sporozoa. Eur J Protistol **50**:472–495

Chobotar B, Scholtyseck E (1982) Ultrastructure. In Long PL (ed) The Biology of the Coccidia. University Park Press, BaltimoreUniversity Park Press, Baltimore, pp 101–165

Clopton RE (2009) Phylogenetic relationships, evolution, and systematic revision of the septate gregarines (Apicomplexa: Eugregarinorida: Septatorina). Comp Parasitol **76**:167–190

Cook TJP, Janovy J, Clopton RE (2001) Epimerite-host epithelium relationships among eugregarines parasitizing the damselflies *Enallagma civile* and *Ischnura verticalis*. J Parasitol **87**:988–996

Coulon P, Jangoux M (1987) Gregarine species (Apicomplexa) parasitic in the burrowing echinoid *Echinocardium cordatum*: occurrence and host reaction. Dis Aquat Org **2**:135–145

Coulon P, Jangoux M (1988) Coelomocyte Reaction Against *Lithocystis schneideri* (Apicomplexa: Sporozoea), a Gregarine Parasite of the Spatangoid Echinoid *Echinocardium cordatum*. In Burke RD, Mladenov PV, Lambert P, Parsley RL (eds) Echinoderm Biology. Rotterdam, Balkerna, pp 769–773

Coulon P, Jangoux M (1991) Cyclic occurrence of gregarine trophozoites (Apicomplexa) in the burrowing echinoid *Echinocardium cordatum* (Echinodermata, Spatangoidea). Dis Aquat Org **12**:71–73

Corbel JC, Desportes I, Théodoridès J (1979) Étude de *Gonospora beloneides* (Ming.) (=*Lobianchella beloneides* Ming.) (grégarine Urosporidae), parasite coelomique d'une Alciopidae (Polychaeta) et remarques sur d'autres grégarines d'Alciopidae. Protistologica **15**:55–65

Desportes I, Schrével J (eds) The Gregarines. The Early Branching Apicomplexa. Treatise on Zoology - Anatomy, Taxonomy, Biology. Brill, Leiden, Boston, pp 781

Desportes I, Vivarès C, Théodoridès J (1977) Intérêt taxonomique de l'ultrastructure épicytaire chez *Ganymedes* Huxley, *Porospora* Schneider et *Thiriotia* n. g., grégarines parasites de crustacés. Ann Sci Nat Zool **19**:261–277

De Ridder C, Jangoux M (1984) Intracoelomic parasitic Sporozoa in the burrowing spatangoid, *Echinocardium cordatum*: coelomocyte reaction and formation of brown bodies. Helgoländer Meeresunters **37**:225–231

Dogiel V (1906) Beiträge zur Kenntnis der Gregarinen. I. *Cystobia chiridotae* nov. sp. II. *Hyalosphaera gregarinicola* nov. gen. nova spec. Arch Protistenkd **7**:106–130

Dogiel V (1909) Beiträge zur Kenntnis der Gregarinen. III. Über die Sporocysten der Cölom-Monocystideae. Arch Protistenkd **16**:194–208

Dogiel V (1910) Beiträge zur Kenntnis der Gregarinen. IV. *Callynthrochlamys phronimae* Frenz. u. a. m. Arch Protistenkd **20**:60–78

Durchon M, Vivier E (1961) Déterminisme de la gamogonie chez une Grégarine parasite de *P. cultrifera* G. (Annelide Polychète). C R Acad Sci Paris **253**:318–320

Dyakin AY, Paskerova GG (2004) *Urospora chiridotae* (Sporozoa: Gregarinomorpha: Eugregarinida) – a neogamic parasite of sea cucumber *Chiridota laevis* (Echinodermata: Holothuroidea: Apoda). Parazitologiya **38**:225–238 (in Russian with English summary)

Dyakin AY, Simdyanov TG (2005) The cortical zone of skittle-like cells of *Urospora chiridotae*, a gregarine from an apode holothuria *Chiridota laevis*. Protistology **4**: 97–105

Edgar RC (2004) MUSCLE: multiple sequence alignment with high accuracy and high throughput. Nucleic Acids Res **35**:1792–1797

Felsenstein J (1985) Confidence limits on phylogenies: an approach using the bootstrap. Evolution **39**:783–791

Frolov AO (1991) World fauna of gregarines. Family Monocystidae. Zool Inst Acad Sci USSR, Leningrad (in Russian with English summary)

Grassé PP (1953) Classe des Grégarinomorphes. In Grassé P-P (ed) Traité de Zoologie. Masson, Paris, pp 550–690

Hall TA (1999) BioEdit: a user-friendly biological sequence alignment editor and analysis program for Windows 95/98/NT. Nucleic Acids Symp Ser **41**:95–98

Hildebrand HF (1981) Elektronenmikroskopische Untersuchungen an den Entwicklungsstadien des Trophozoiten von *Didymophyes gigantea* (Sporozoa, Gregarinida). 3. Die Feinstruktur des Epizyten mit besonderer Berücksichtigung der kontraktilen Elemente. Z Parasitenkd **64**:29–46

Jobb G (2011) TREEFINDER version of March 2011. 2011. Munich, Germany. Distributed by the author at www.treefinder.de

Jobb G, von Haeseler A, Strimmer K (2004) TREEFINDER: A powerful graphical analysis environment for molecular phylogenetics. BMC Evol Biol **4**:18, http://dx.doi.org/10.1186/1471-2148-4-18

King CA (1981) Cell surface interaction of the protozoa Gregarina with concanavalin A beads. Implications for models for gregarine gliding. Cell Biol Int Rep **5**:297–305

King CA (1988) Cell motility of sporozoan protozoa. Parasitol Today **4**:297–305

Kishino H, Hasegawa M (1989) Evaluation of the maximum likelihood estimate of the evolutionary tree topologies from DNA sequence data, and the branching order in hominoidea. J Mol Evol **29**:170–179

Landers SC (1991) *Pterospora demodendrion* sp. nov. and *Pterospora clymenellae*, acephaline eugregarines from coastal North Carolina. Eur J Protistol **27**:55–59

Landers SC (2001) *Pterospora floridiensis*, a new species of acephaline gregarine (Apicomplexa) from the maldanid polychaete *Axiothella mucosain* St. Andrew Bay, Florida. Syst Parasitol **48**:55–59

Landers SC (2002) The fine Structure of the Gamont of *Pterospora floridiensis* (Apicomplexa: Eugregarinida). J Eukaryot Microbiol **49**:220–226

Landers SC, Gunderson J (1986) *Pterospora schizosoma*, a new species of aseptate gregarine from the coelom of *Axiothella rubrocincta* (Polychaeta, Maldanidae). J Protozool **33**:297–300

Landers SC, Leander BS (2005) Comparative surface morphology of marine coelomic gregarines (Apicomplexa,

Urosporidae): *Pterospora floridiensis* and *Pterospora schizosoma*. J Eukaryot Microbiol **52**:23–30

Leander BS (2008) Marine gregarines: evolutionary prelude to the apicomplexan radiation? Trends Parasitol **24**:60–67

Leander BS, Lloyd SAJ, Marshall W, Landers SC (2006) Phylogeny of marine gregarines (Apicomplexa) — *Pterospora*, *Lithocystis* and *Lankesteria* — and the origin(s) of coelomic parasitism. Protist **157**:45–60

Levine ND (1977) Checklist of the species of the aseptate gregarine family Urosporidae. Int J Parasitol **7**:101–108

Léger L (1892) Recherches sur les Grégarines. Tablettes Zoologiques **3**:1–182

Long PL (ed) The Biology of the Coccidia. Edward Arnold Press, London, pp 502

Mackenzie C, Walker MH (1983) Substrate contact, mucus, and eugregarines gliding. J Protozool **30**:3–8

MacMillan WG (1973) Conformation changes in the cortical region during peristaltic movements of a gregarine trophozoite. J Protozool **20**:267–274

Miles HB (1968) The fine structure of the epicyte of the acephaline gregarines *Monocystis lumbrici-olidi*, and *Nematocystis magna*: observations by electron microscope. Rev Iber Parasitol **28**:455–465

Mita K, Kawai N, Rueckert S, Sasakura Y (2012) Large-scale infection of the ascidian *Ciona intestinalis* by the gregarine *Lankesteria ascidiae* in an inland culture system. Dis Aquat Org **101**:185–195

Perkins FO, Barta JR, Clopton RE, Peirce MA, Upton SJ (2000) Phylum Apicomplexa Levine, 1970. In Lee JJ, Leedale GF, Bradbury P (eds) An Illustrated Guide to the Protozoa **Vol 1**, 2nd edn Society of Protozoologists, Lawrence, Kansas, USA, pp 190–369

Philippe M, Schrével J (1982) The three cortical membranes of the gregarines (parasitic protozoa). Characterization of the membrane proteins of *Gregarina blaberae*. Biochem J **201**:455–464

Pixell-Goodrich H (1915) On the life-history of the sporozoa of spatangoids, with observations on some allied forms. Quart J Microsc Sci **61**:84–106

Pixell-Goodrich H (1950) Sporozoa of *Sipunculus*. Quart J Microsc Sci **91**:469–476

Pomory CM, Lares MT (1998) *Gonospora holoflora* - a new species of gregarine protozoan parasite (Apicomplexa) in *Holothuria floridana* (Echinodermata, Holothuroidea) from the Florida-Keys. Bull Marine Sci **62**:213–218

Porchet E (1978) Etude de cinq sporozoaires parasitant un meme hote: l'annelide polychaete *Notomastus latericeus*. Protistologica **14**:59–76

Reynolds ES (1963) The use of lead citrate at high pH as an electron opaque stain in electron microscopy. J Cell Biol **17**:208–212

Ronquist F, Huelsenbeck JP (2003) MrBayes 3: Bayesian phylogenetic inference under mixed models. Bioinformatics **19**:1572–1574

Rueckert S, Chantangsi C, Leander BS (2010) Molecular systematics of marine gregarines (Apicomplexa) from Northeastern Pacific polychaetes and nemerteans, with descriptions of three novel species: *Lecudina phyllochaetopteri* sp. nov., *Difficilina tubulani* sp. nov. and *Difficilina paranemertis* sp. nov. Int J Syst Evol Microbiol **60**:2681–2690

Rueckert S, Villette PM, Leander BS (2011b) Species boundaries in gregarine apicomplexan parasites: a case study-comparison of morphometric and molecular variability in Lecudina cf. tuzetae (Eugregarinorida, Lecudinidae). J Eukaryot Microbiol **58**:275–283

Rueckert S, Simdyanov TG, Aleoshin VV, Leander BS (2011a) Identification of a divergent environmental DNA sequence clade using the phylogeny of gregarine parasites (Apicomplexa) from crustacean hosts. PLoS ONE **6**:e18163, http://dx.doi.org/10.1371/journal.pone.0018163

Rueckert S, Wakeman KS, Holger Jenke-Kodama H, Leander BS (2015) Molecular systematics of marine gregarine apicomplexans from Pacific tunicates, with descriptions of five novel species of *Lankesteria*. Int J Syst Evol Microbiol **65**:2598–2614

Scholtyseck E (1973) Ultrastructure. In Hammond DM, Long PL (eds) The Coccidia: *Eimeria, Isospora, Toxoplasma*, and Related Genera. University Park Press, Baltimore, MD, pp 81–144

Scholtyseck E, Mehlhorn H (1970) Ultrastructural study of characteristic organelles (paired organelles, micronemes, micropores) of Sporozoa and related organisms. Z Parasitenkd **34**:97–127

Schrével J (1964) Contribution à l'étude de trois Grégarines parasites d'Annélides Polychètes: *Lecudina elongata* Mingazzini, 1891; *Lecudina tuzetae* Schrével, 1963; *Gonospora varia* Léger, 1892. Arch Zool exp gén **104**:125–142

Schrével J (1971a) Contribution à l'étude à l'étude des selenidiidae parasites d'annélides Polychètes: II. ultrastructure de quelques trophozoites. Protistologica **7**:101–130

Schrével J (1971b) Observations biologiques et ultrastructurales sur les Selenidiidae et leurs consequences sur la systematique des Gregarinomorphes. J Protozool **18**:448–470

Schrével J, Caigneaux E, Gros D, Philippe M (1983) The three cortical membranes of the gregarines. I. Ultrastructural organization of *Gregarina blaberae*. J Cell Sci **61**:151–174

Shimodaira H (2002) An approximately unbiased test of phylogenetic tree selection. Syst Biol **51**:492–508

Shimodaira H, Hasegawa M (1999) Multiple comparisons of log-likelihoods with applications to phylogenetic inference. Mol Biol Evol **16**:1114–1116

Siedlecki M (1903) Quelques observations sur les rôles des amibocytes dans le coelome d'une Annélide. Ann Inst Pasteur **17**:449–462

Simdyanov TG (1995a) An ultrastructure of two species of gregarines of the genus *Lankesteria* (Eugregarinida: Lecudinidae). Parazitologiya **29**:424–432 (in Russian with English summary)

Simdyanov TG (1995b) Two new species of gregarines with the aberrant structure of epicyte from the White Sea. Parazitologiya **29**:305–315 (in Russian with English summary)

Simdyanov TG (2009) *Difficilina cerebratuli* gen. et sp. n. (Eugregarinida: Lecudinidae) - a new gregarine species from the nemertean *Cerebratulus barentsi* (Nemertini: Cerebratulidae). Parazitologiya **43**:273–287 (In Russian with English summary)

Simdyanov TG, Diakin AY, Aleoshin VV (2015) Ultrastructure and 28S rDNA phylogeny of two gregarines: *Cephaloidophora* cf. *communis* and *Heliospora* cf. *longissima* with remarks on gregarine morphology and phylogenetic analysis. Acta Protozool **54**:241–263

Stamatakis A (2006) RAxML-VI-HPC: maximum likelihood-based phylogenetic analyses with thousands of taxa and mixed models. Bioinformatics **22**:2688–2690

Strimmer K, Rambaut A (2002) Inferring confidence sets of possibly mis-specified gene trees. Proc R Soc Lond B **269**:137–142

Valigurová A (2012) Sophisticated adaptations of *Gregarina cuneata* (Apicomplexa) feeding stages for epicellular parasitism. PLoS ONE **7**:e42606, http://dx.doi.org/10.1371/journal.pone.0042606

Valigurová A, Vaškovicová N, Musilová N, Schrével J (2013) The enigma of eugregarine epicytic folds: where gliding motility originates? Front Zool **10**:57, http://dx.doi.org/10.1186/1742-9994-10-57

Vávra J, Small EB (1969) Scanning electron microscopy of gregarines (Protozoa, Sporozoa) and its contribution to the theory of gregarine movement. J Protozool **16**:745–757

Vegni Talluri M, Dallai R (1983) Freeze-fracture study of the gregarine trophozoite: II. Evidence of "rosette" organization on cytomembranes in relation with micropore structure. Boll Zool **50**:245–255

Vinckier D (1969) Organisation ultrastructurale corticale de quelques Monocystidées parasites du ver Oligochète *Lumbricus terrestris* L. Protistologica **5**:505–517

Vinckier D, Vivier E (1968) Organisation ultrastructurale corticale de la Grégarine *Monocystis herculea*. C R Acad Sci D **266**:1737–1739

Vivier E (1968) L'organisation ultrastructurale corticale de la Grégarine *Lecudina pellucida*; ses rapports avec l'alimentation et la locomotion. J Protozool **5**:230–246

Vivier E, Devauchelle G, Petitprez A, Porchet-Henneré E, Prensier G, Schrével J, Vinckier D (1970) Observations de cytologie comparée chez les Sporozoaires. I.- Les structures superficielles chez les formes végétatives. Protistologica **6**:127–150

Wakeman KC, Leander BS (2012) Molecular phylogeny of pacific archigregarines (Apicomplexa), including descriptions of *Veloxidium leptosynaptae* n. gen., n. sp., from the sea cucumber *Leptosynapta clarki* (Echinodermata), and two new species of *Selenidium*. J Eukaryot Microbiol **59**:232–245

Wakeman KC, Reimer JD, Jenke-Kodama H, Leander BS (2014) Molecular phylogeny and ultrastructure of *Caliculium glossobalani* n. gen. et sp. (Apicomplexa) from a Pacific *Glossobalanus minutus* (Hemichordata) confounds the relationships between marine and terrestrial gregarines. J Eukaryot Microbiol **61**:343–353, http://dx.doi.org/10.1111/jeu.12114

Walker MH, Lane NJ, Lee WM (1984) Freeze-fracture studies on the pellicle of the eugregarine, *Gregarina garnhami* (Eugregarinida, Protozoa). J Ultrastruct Res **88**:66–76

Warner FD (1968) The fine structure of *Rhynchocystis pilosa* (Sporozoa, Eugregarinida). J Protozool **15**:59–73

Available online at www.sciencedirect.com

ScienceDirect